A polynomial upwind scheme for convection discretization

Rafael A. B. de Queiroz[*], **Fernando A. Kurokawa**, **Valdemir G. Ferreira**
Departamento de Matemática Aplicada e Estatística, ICMC, USP
Av. Trabalhador São-Carlense, 400 - Centro, São Carlos, SP
Caixa Postal: 668 - CEP: 13560-970
E-mail: bonfim@icmc.usp.br, kurokawa@icmc.usp.br, pvgf@icmc.usp.br

Abstract: *The objective of this work is to present the development and assessment of a polynomial upwind scheme for convection terms discretization. The performance of this new upwind strategy is investigated in 1D applications dominated by convection. The numerical results obtained are quite consistents with the analytical solutions and demonstrate that second order of accuracy is achieved in these 1D problems.*

Keywords: polynomial upwind schemes, convective transport, numerical simulation.

1 Introduction

The development of numerical schemes to estimate convective terms in partial differential equations of predominantly convective character has been subject of intense research in the last years by modern scientific community in computational fluid dynamics. In the process of numerically solving of these equations, the precision of the results is, significantly, affected by the choice of the convection scheme.

Inside of this context, a polynomial upwind scheme called TOPUS (Third-Order Polynomial Upwind Scheme) [11] is proposed. Such a scheme determines a family of third-order accurate polynomial upwind schemes, whose principal purpose is to simulate predominantly convective fluid fluxes. The construction of this scheme is based on NVD (Normalized Variable Diagram) restrictions of Leonard [8], and by enforcing the TVD (Total Variation Diminishing) constraints of Harten [6] (see also Sweby [12]). Consequently, it satisfies the CBC (Convection-Boundedness Criterion) criterion of Gaskell and Lau [5]. In addition, the flux limiter [14] is also obtained for the TOPUS.

The assessment and performance of this new upwind strategy is investigated by using the Euler equations [13, 15], the viscous Burgers equation [1, 3] and the boundary layer problem [3]. These 1D problems have been important tests in the literature to analyse the performance of convection schemes.

The organization of this investigation is as follows. In Section 2, a short outline of normalized variable and criterion CBC is presented. In Section 3, the mathematical formulation of the TOPUS scheme is described. In Section 4, some numerical 1D test problems and their numerical solutions are presented. Section 5 contains our conclusions and discusses the future direction of this work.

2 Normalized Variable

Given $\phi(x, y)$ the variation of one scalar in the normal direction to the f face as shown in Figure 1. In this figure, the D (*Downstream*), U (*Upstream*) and R (*Remote-Upstream*) positions are determined according to V_f convecting velocity at the f interface. In order to facilitate the analysis of the functional relationship linking ϕ_D, ϕ_U and ϕ_R, the original variables are transformed in normalized variables (NV) of Leonard [8] as

$$\hat{\phi} = \frac{\phi - \phi_R}{\phi_D - \phi_R}. \tag{1}$$

The advantage of the NV formulation is that the interface value $\hat{\phi}_f$ depends on $\hat{\phi}_U$ only, since $\hat{\phi}_D = 1$ and $\hat{\phi}_R = 0$.

Leonard [8] showed that any NV scheme (in general non-linear) that passes on the point

[*] bolsista de Mestrado - FAPESP

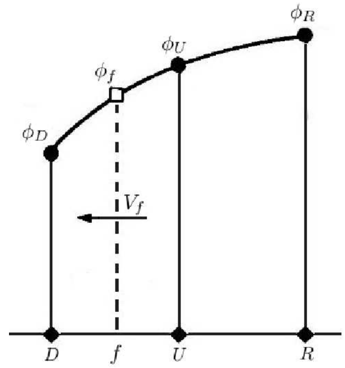

Figure 1: Original variables [11].

$Q(0.5, 0.75)$ of the NVD (see Figure 3) is a necessary and sufficient condition to reach second order of accuracy, and any scheme that passes on the point Q with inclination 0.75 is a necessary and sufficient condition for third order accurate. Leonard [8] also recommended that for values of $\hat{\phi}_U$ less than 0 and greater than 1, the scheme must be continued on continuous way with the FOU (First-Order Upwind) scheme defined as $\hat{\phi}_f = \hat{\phi}_U$.

2.1 CBC Criterion

Gaskell and Lau [5] proposed the CBC criterion for an advective scheme to possess the boundedness property. Convection schemes based on CBC predict bounded solutions. The CBC region in the NVD of Leonard is shown in Figure 2. A short outline of CBC is as follows.

Given a continuous or piecewise continuous NV characteristic $\hat{\phi}_f = \hat{\phi}_f\left(\hat{\phi}_U\right)$, it possesses the monotonicity-preserving (boundedness) if and only if the following conditions are satisfied

- $\forall \hat{\phi}_U \in [0, 1], \quad \hat{\phi}_U \leq \hat{\phi}_f(\hat{\phi}_U) \leq 1;$
- $\forall \hat{\phi}_U \notin [0, 1], \quad \hat{\phi}_f = \hat{\phi}_f(\hat{\phi}_U) = \hat{\phi}_U;$
- $\hat{\phi}_f(0) = 0$ and $\hat{\phi}_f(1) = 1$.

3 TOPUS scheme

Various monotone schemes have been proposed using simple polynomial functions in the CBC region, passing through the three critical points: $O(0, 0)$, $Q(0.5, 0.75)$ and $P(1, 1)$ (see Figure 3). Such polynomials of order n in NV form transform into polynomial-ratio limiters of order $(n-1)$ in the limiter formulation [14]. Zhu [16] proposed a quadratic fit denoted by HLPA (Hybrid - Linear Parabolic Approximation), while different authors [2, 9, 17, 18, 19] have proposed the same cubic polynomial under a variety of names tangential to the QUICK at $\hat{\phi}_U = 0.5$, that was referred as SMARTER by Waterson et al. [14].

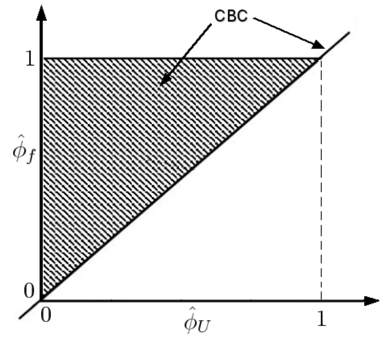

Figure 2: CBC region in $\hat{\phi}_f$– $\hat{\phi}_U$ plane.

The SMARTER violated the Sweby's monotonicity preservation condition [12]. This can be expected, because the CBC is weaker and thus more flexible than Sweby's TVD criterion [19]. Besides, it is not entirely contained in the Harten's TVD region [6].

In the construction of the monotone TOPUS scheme, we use CBC criterion and the recommendations of Leonard argued above. These conditions of Leonard plus a free variable were used for its derivation

$$\hat{\phi}_f = \alpha\hat{\phi}_U^4 + (-2\alpha + 1)\,\hat{\phi}_U^3 + \left(\frac{5\alpha - 10}{4}\right)\hat{\phi}_U^2 + \left(\frac{-\alpha + 10}{4}\right)\hat{\phi}_U, \quad (2)$$

where $-2 \leq \alpha \leq 2$ ensures that the TOPUS scheme satisfies the CBC criterion and $\hat{\phi}_U \in [0, 1]$. For $\hat{\phi}_U \notin [0, 1]$, the TOPUS scheme get $\hat{\phi}_f = \hat{\phi}_U$. If $\alpha = 2$ in equation (2), it determines that the scheme is entirely contained in the TVD region [6] (see Figure 3) and its corresponding flux limiter $\psi(r_f)$ satisfied the Sweby's monotonicity preservation condition when r_f tend to 0 (see equation (5)). If $\alpha = 0$ in equation (2), it generates the SMARTER scheme [14].

It is important to inform the reader that the TOPUS is a generalisation of the upwind polynomial scheme ("Esquema II") constructed by Queiroz et al. [10].

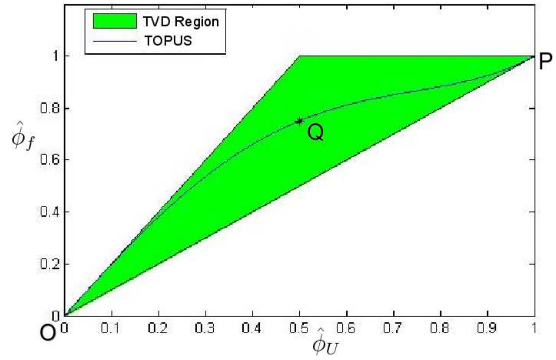

Figure 3: TOPUS with $\alpha = 2$ in the region TVD.

The flux limiter of the TOPUS scheme defined in equation (2) is deduced rewriting it as

$$\hat{\phi}_f = \hat{\phi}_U + \frac{1}{2}\psi(r_f)(1 - \hat{\phi}_U), \qquad (3)$$

where ψ is the flux limiter, that determines the anti-diffuse level, and r_f is ratio between two consecutive gradients defined in NV as

$$r_f = \frac{\hat{\phi}_U}{1 - \hat{\phi}_U}. \qquad (4)$$

From equations (2), (3) and (4), one deduces that the flux limiter for the TOPUS is

$$\psi(r_f) = \frac{0.5\,(|r_f| + r_f)\,P^{\alpha}}{(1 + |r_f|)^3}, \qquad (5)$$

where P^{α} is given by

$$P^{\alpha} = (-0.5\alpha+1)r_f^2 + (\alpha+4)r_f + (-0.5\alpha+3). \qquad (6)$$

The flux limiter (5) has the advantage of being a smooth function of r_f for $r_f > 0$, so it may offer the best convergence behavior [19].

In this work, it is analyzed the TOPUS with $\alpha = 2$ given by

$$\hat{\phi}_f = \begin{cases} 2\hat{\phi}_U^4 - 3\hat{\phi}_U^3 + 2\hat{\phi}_U, & \hat{\phi}_U \in [0,1], \\ \hat{\phi}_U, & \hat{\phi}_U \notin [0,1]. \end{cases}$$

and its flux limiter is defined as

$$\psi(r_f) = \frac{(r_f + |r_f|)\,(3r_f + 1)}{(|r_f| + 1)^3}.$$

4 Numerical Results

In this section, we examine the performance of the TOPUS by solving the following 1D problems, namely: shock tube, viscous Burgers equation and boundary layer.

4.1 Shock Tube

The shock tube problem is a very interesting test case because its time-dependent solution is known and can be compared with the computed solution using numerical methods. The initial solution for this problem is composed by two uniform states separated by a discontinuity which is usually located at the origin. This particular initial value problem is well known as Riemann problem. The initial left and right uniform states are usually introduced by giving the density, the pressure and the velocity.

This problem is used in the experimental investigation of several physical phenomena, such as chemical reaction kinetics, shock structure, and aero-thermodynamics of supersonic/hypersonic vehicles [7]. Moreover, this problem is very useful for assessing the entropy satisfaction property of numerical method [13].

The conservation law that models the shock tube problem is the 1D Euler equations, which take the form

$$\frac{\partial \mathbf{U}}{\partial t} + \frac{\partial \mathbf{F}(\mathbf{U})}{\partial x} = 0, \qquad (7)$$

with $\mathbf{U} = (\rho, \rho v, E)^T$, $\mathbf{F}(\mathbf{U}) = (\rho v, \rho v^2 + p, v(E+p))^T$. The variables ρ, v, p and E are the density, velocity, pressure, and the total energy per unit volume respectively, with $p = (\gamma - 1)[E - \rho v^2/2]$, where γ is the ratio of ratio specific heats that assumes the usual value of 1.4.

We consider two well known Riemann problems [13], which are designed to assess the robustness and accuracy of numerical schemes.

- **Test Problem 1:** The first test case is formulated by equation (7) with the initial condition given by

$$(\rho, v, p)^T = \begin{cases} (1, 0, 1000)^T, & x < 0.5, \\ (1, 0, 0.01)^T, & x \geq 0.5. \end{cases}$$

The solution of this problem consists of a strong shock wave, a contact surface and a left rarefaction wave. This test is actually the left half of the blast wave problem of Woodward and Colella [15].

Figures 4 and 5 show the reference solution (continuous red line) and the numerical results (blue symbols) for density produced by TOPUS scheme. In the simulation, it was used a uniform mesh of 800 computational cells over $0 \leq x \leq 1$, two Courant numbers ($\theta = 0.2$ and $\theta = 0.6$) and time $t = 0.012$. One can seen from these figures that the TOPUS provided good results for both the values of θ.

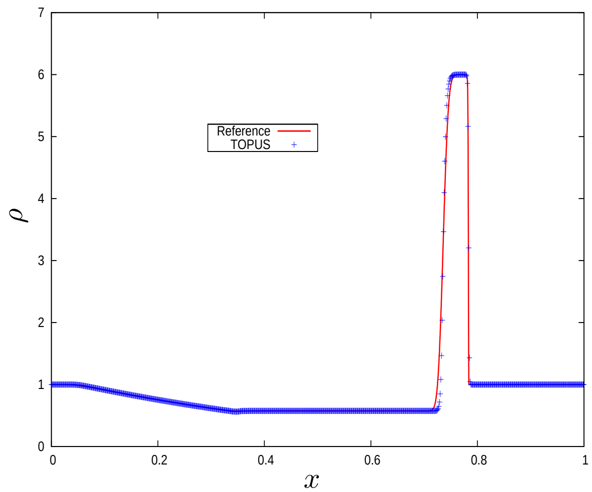

Figure 4: Results for density (ρ) of the shock tube problem with $\theta = 0.2$.

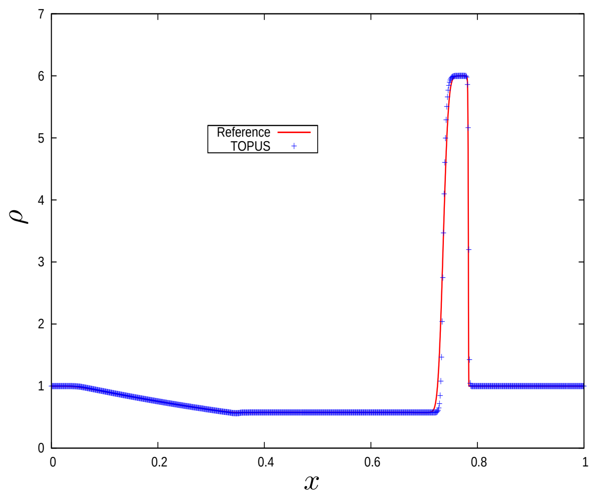

Figure 5: Results for density (ρ) of the shock tube problem with $\theta = 0.6$.

- **Test Problem 2:** The second test case selected is formulated by equation (7) with $0 \leq x \leq 1$ and initial condition $(\rho, v, p)^T$ is given by

$$\begin{cases} (5.99924, 195975, 460.894)^T, & x < 0.4, \\ (5.99242, -6.19633, 46.0950)^T, & x \geq 0.4. \end{cases}$$

The solution of this test consists of three strong discontinuities traveling to the right. Figures 6 and 7 depict the numerical results for density obtained with the TOPUS scheme. The uniform mesh used for this problem was the 800 computational cells, time $t = 0.035$ and Courant numbers $\theta = 0.2$ and $\theta = 0.6$. Once again, for this problem, one can be seen from these figures that the TOPUS scheme provides a satisfactory solution.

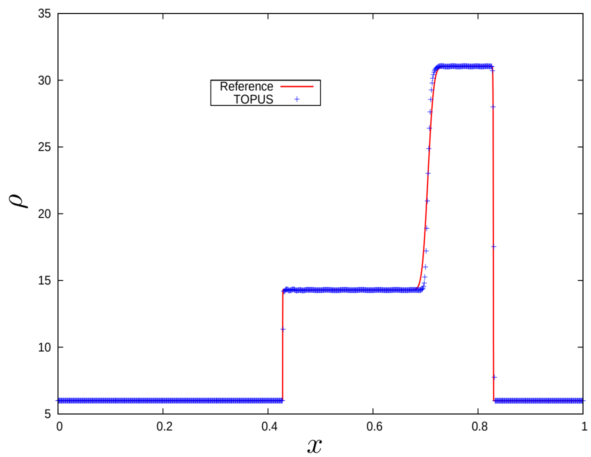

Figure 6: Results for density (ρ) of the shock tube problem with $\theta = 0.2$.

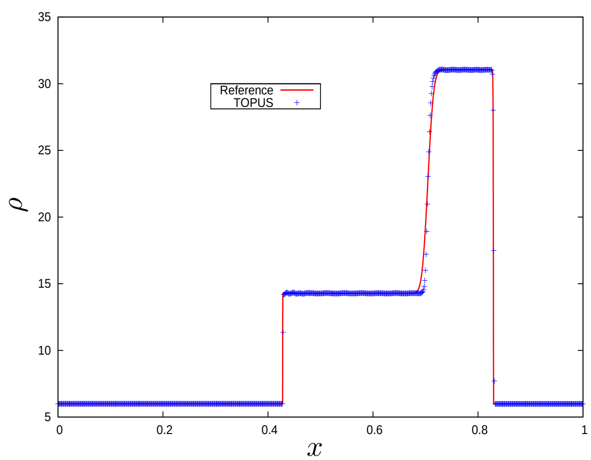

Figure 7: Results for density (ρ) of the shock tube problem with $\theta = 0.6$.

4.2 Viscous Burgers equation

The viscous Burgers problem (non-linear) is given by

$$\begin{cases} u_t + \left(\frac{u^2}{2}\right)_x = \frac{1}{Re} u_{xx}, & 0 < x < 1, \\ u(0,t) = +\alpha, & t \geq 0, \\ u(1,t) = -\alpha, & t \geq 0. \end{cases} \quad (8)$$

In equation (8), the α coefficient is chosen equal to $tanh(0.25Re)$ according to Corre and Lerat [3], where Re denotes the Reynolds number. This equation admits $u(x) = tanh\left(0.5Re\left(0.5 - x\right)\right)$ as the exact steady state solution. The initial condition for (8) is defined as $u(x,0) = tanh\left(0.5Re\left(0.5 - x\right)\right)$, $0 \leq x \leq 1$.

Tables 1 and 2 show the order of accuracy of TOPUS scheme for this test case using $Re = 20$ and $Re = 100$, respectively. Note that the solution of (8) is obtained on a series of increasingly refined grids (from $N = 50$ up to $N = 800$).

N	L_1 order	L_2 order	L_∞ order
50	–	—	–
100	1.704	1.794	1.864
200	1.864	1.901	1.934
400	1.941	1.949	1.952
800	1.982	1.969	1.934

Table 1: Convergence test: L_1, L_2 and L_∞ orders estimate for the TOPUS scheme using $Re = 20$.

N	L_1 order	L_2 order	L_∞ order
50	–	—	–
100	0.957	0.745	0.438
200	1.324	1.556	1.771
400	1.625	1.749	1.802
800	1.836	1.877	1.911

Table 2: Convergence test: L_1, L_2 and L_∞ orders estimate for the TOPUS scheme using $Re = 100$.

Figure 8 illustrates the exact solution and numerical results obtained with the TOPUS using 100 computational cells, $Re = 20$ and $Re = 100$. As it can be seen from this figure, the numerical and analytical solutions are in good agreement.

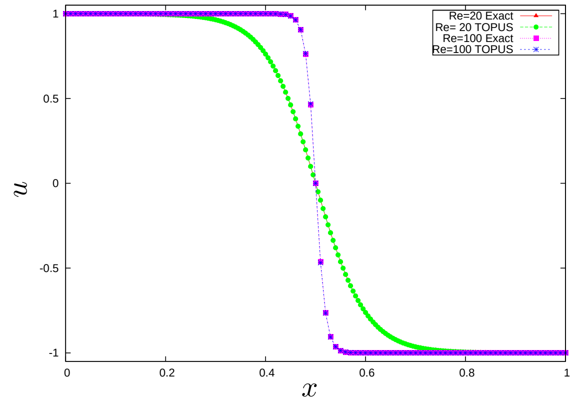

Figure 8: Numerical and analytic (Exact) solutions for the 1D Burgers equation using 100 computational cells, $Re = 20$ and $Re = 100$.

4.3 Boundary layer

This 1D viscous flow model problem [3] is defined as

$$\begin{cases} u_t + a u_x = \frac{1}{Re} u_{xx}, & 0 < x < L; \\ u(x,0) = 0, & 0 \leq x \leq L; \\ u(0,t) = 1, & t \geq 0; \\ u(L,t) = 1, & t \geq 0; \end{cases} \quad (9)$$

The exact solution of the equation (9) on a N computational cells $((i\delta x)_{(0 \leq i \leq N)})$ is given by [3]: $u_i = (1 - exp(iRe_\delta))/(1 - exp(Re))$, where $Re = aL/\nu$. The $Re_\delta = a\delta_x/\nu = Re/N$ denotes the cell Reynolds number, where ν is the diffusion coefficient. In this study, a and L are fixed to unity.

Tables 3 and 4 show the rate of convergence of the TOPUS scheme for this problem using $Re = 50$ and $Re = 100$, respectively. Note that the solution of the equation (9) is obtained on a series of increasingly refined grids (from $N = 80$ up to $N = 640$).

N	L_1 order	L_2 order	L_∞ order
80	–	—	–
160	2.107	2.137	2.298
320	2.256	2.248	2.338
640	2.391	2.313	2.268

Table 3: Convergence test: L_1, L_2 and L_∞ orders estimate for the TOPUS scheme using $Re = 50$.

Figure 9 illustrates the exact solution and numerical results obtained with the TOPUS.

N	L_1 order	L_2 order	L_∞ order
80	–	—	–
160	1.584	1.667	2.013
320	2.100	2.135	2.294
640	2.215	2.222	2.344

Table 4: Convergence test: L_1, L_2 and L_∞ orders estimate for the TOPUS scheme using $Re = 100$.

These results are very similar to those obtained by Corre and Lerat [3].

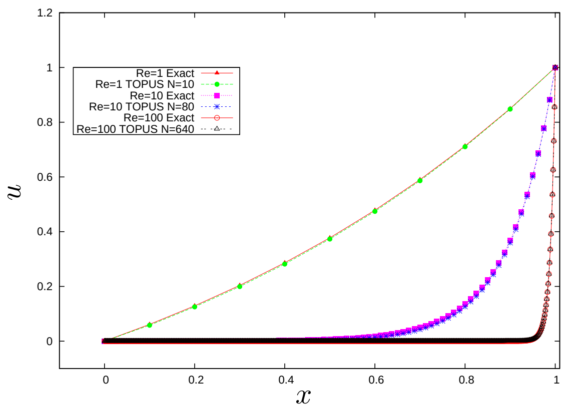

Figure 9: Numerical and analytic (Exact) solutions for the 1D boundary layer.

5 Conclusions and Future Works

In this work, we presented the development and assessment of the TOPUS scheme for convection terms discretization. The numerical results confirm the ability of this high order upwind scheme for approximating advection terms in 1D conservation laws.

Some possibilities for future works are to investigate the performance of the TOPUS scheme in solving 2D/3D turbulent and non-Newtonian incompressible free surface flows [4].

Acknowledgments

This research work was supported by the *FAPESP* under Grants 04/16064-9, 05/51458-0, 06/05910-1 and *CNPq* under Grant 304201/05-7.

References

[1] J. M. Burgers, A mathematical model illustrating the theory of turbulence, *Advances in Applied Mechanics*, 1 (1948) 171-199.

[2] S. K. Choi, H. Y. Nam and M. Cho, A comparison of higher-order bounded convection schemes, *Computer Methods in Applied Mechanics and Engineering*, 121 (1995) 281.

[3] C. Corre and A. Lerat, High-order residual-based compact schemes for advection-diffusion problems, *Computers & Fluids*, 37 (2008) 505-519.

[4] V. G. Ferreira, C. M. Oishi, F. A. Kurokawa, M. K. Kaibara, J. A. Cuminato, A. Castelo, M. F. Tomé and S. Mckee, A combination of implicit and adaptative upwind tools for numerical solution of incompressible free surface flows, *Comunications in Numerical Methods in Engineering*, 23 (2007) 419-445.

[5] P. H. Gaskell and A. K. C. Lau, Curvature-compensated convective transport: SMART, a new boundedness-preserving transport algorithm, *International Journal for Numerical Methods in Fluids*, 8 (1988) 617-641.

[6] A. Harten, High resolution schemes for conservation laws, *Journal of Computational Physics*, 49 (1983) 357-393.

[7] C. B. Laney, "Computational Gasdynamics", Cambridge University Press, 1998.

[8] B. P. Leonard, Simple high-accuracy resolution program for convective modeling of discontinuities, *International Journal for Numerical Methods in Fluids*, 8 (1988) 1291-1318.

[9] A. Pascau, C. Perez, A well-behaved scheme to model strong convection in a general transport equation, in: Taylor (Ed.), Proceedings of the Eighth International Conference on Numerical Methods in Laminar and Turbulent Flow, Swansea, July, Pineridge Press, Swansea, 1993.

[10] R. A. B. Queiroz, V. G. Ferreira and F. A. Kurokawa, Desenvolvimento e aplicação de esquemas upwind de terceira ordem para transporte convectivo, *XXX Congresso Nacional de Matemática Aplicada e Computacional - XXX CNMAC*, Florianópolis - SC, 2007.

[11] R. A. B. Queiroz, R. G. Cuenca, V. G. Ferreira and L. F. Souza, A new high resolution TVD scheme for unsteady flows with shock waves, *Proceedings of the 7th Brazilian Conference On Dynamics, Control and Applications - DINCON*, Presidente Prudente-SP, 2008.

[12] P. K. Sweby, High resolution scheme using flux limiters for hyperbolic conservation laws, *SIAM Journal on Numerical Analysis*, 21 (1984) 995-1011.

[13] E. F. Toro, "Riemann Solves and Numerical Methods for Fluid Dynamics", 2nd Edition Springer-Verlag, Berlin, Heidelberg, 1999.

[14] N. P. Waterson, H. Deconinck, Design principles for bounded higher-order convection schemes - a unified approach, *Journal of Computational Physics*, 224 (2007) 182-207.

[15] P. Woodward and P. Colella, The numerical simulation of two-dimensional fluid flow with strong shocks, *Journal of Computational Physics*, 24 (1984) 115-173.

[16] J. Zhu, On the higher-order bounded discretization schemes for finite volume computations of incompressible flows, *Computer Methods in Applied Mechanics and Engineering*, 98 (1992) 345.

[17] G. Zhou, L. Davidson, E. Olsson, Transonic inviscid/turbulent airfoil flow simulations using a pressure-based method with high order schemes, Lecture Notes in Physics, 453 (1995) 372.

[18] M. Zijlema, Computational modeling of turbulent flow in general domains, Doctoral Thesis, Delft University of Technology, The Netherlands, 1996.

[19] M. Zijlema, On the construction of a third-order accurate monotone convection scheme with application to turbulent flows in general domains, *International Journal For Numerical Methods in Fluids*, 22 (1996) 619-641.